

## Supporting Information

### **Integrated Cu<sub>3</sub>N Porous Nanowires Array Electrode for High Performance Supercapacitors**

*Fanlu Meng<sup>a,b</sup>, Haixia Zhong<sup>b</sup>, Qi Zhang<sup>b</sup>, Kaihua Liu<sup>a,b</sup>, Junmin Yan<sup>a\*</sup> and Qing Jiang*

<sup>a</sup>Key Laboratory of Automobile Materials, Ministry of Education and College of Materials Science and Engineering, Jilin University, Changchun 130012, Jilin, China

<sup>b</sup>State Key Laboratory of Rare Earth Resource Utilization, Changchun Institute of Applied Chemistry, Chinese Academy of Sciences, Changchun 130022, Jilin, China

Address correspondence to Junmin Yan, [junminyan@jlu.edu.cn](mailto:junminyan@jlu.edu.cn)

## **Experimental section**

### **Synthesis of samples**

All chemicals used in the experiment were of analytical grade and used without further purification. Cu(OH)<sub>2</sub> nanowires array were first synthesized on Cu foam by immersing Cu foam into a solution mixture containing 0.133 M (NH<sub>3</sub>)<sub>2</sub>S<sub>2</sub>O<sub>8</sub> and 2.667 M NaOH. After 5 minutes, the Cu foam was taken out from the solution, rinsed with de-ionized water and absolute ethanol, and dried with nitrogen. Porous Cu<sub>3</sub>N nanowires array on Cu foam was then fabricated by annealing the Cu(OH)<sub>2</sub> nanowires array at 350 °C for 2 hours in flow NH<sub>3</sub>. For comparison, the CuO nanowires array on Cu foam was also fabricated by annealing the Cu(OH)<sub>2</sub> nanowires array at 150 °C for 2 hours in air.

### **Characterizations**

Scanning electron microscopy (SEM) was performed with a field emission scanning electron microanalyzer (Hitachi S4800) operating at an accelerating voltage of 10 kV. Transmission electron microscope (TEM) and elemental-mapping were performed on a FEI Tecnai G2 S-Twin instrument with a field emission gun operating at 200 kV. Powder X-ray diffraction (XRD) measurement was carried out using an X-ray diffractometer (micro-XRD, Rigaku, Japan) with Cu K $\alpha$  ( $\lambda$ = 0.15406 nm). Nitrogen adsorption-desorption measurements were performed on a Micromeritics ASAP 2020 adsorption analyser. Pore volumes and sizes were estimated from the pore-size distribution curves from the desorption isotherms using the Barrett-Joyner-Halenda (BJH) method. Specific surface areas were calculated by the Brunauer-Emmert-Teller (BET) method. X-ray photoelectron spectroscopy (XPS) analysis was carried on a VG Scientific ESCALAB MKII X-ray photoelectron spectrometer using an Al K $\alpha$  source. All electrochemical measurements were performed on a BioLogic VMP3 electrochemical workstation.

### **Electrochemical measurements**

Electrochemical characterizations were implemented on a VMP3 electrochemical workstation (Bio-Logic Inc.) with a three-electrode system. The Pt foil was used as

the counter electrode and an SCE electrode was used as the reference electrode. All electrochemical measurements were carried out in the 1 M KOH aqueous solution at room temperature. The electrochemical impedance spectroscopy (EIS) was performed in a frequency range from 0.01 Hz to 100 kHz with a 5 mV amplitude at open circuit potential. Before the EIS tests, the fresh samples were activated by CV cycle with a scan rate of 20 mV s<sup>-1</sup> until CV curves almost coinciding.

#### **Assembly of P-Cu<sub>3</sub>N NA/CF//AC asymmetric supercapacitor**

For the asymmetric supercapacitor, the as-prepared P-Cu<sub>3</sub>N NA/CF electrode was directly used for the positive electrode and the active carbon (AC) acted as the negative electrode. The negative electrode was prepared by mixing the AC, carbon black, and poly(tetrafluoroethylene) (PTFE) with ethanol in a mass ratio of 8:1:1. The mixture was dried at 80 °C overnight and then was pressed onto nickel foam. The as-prepared positive electrode and negative electrode were separated by a cellulose paper and were face-to-face placed into an encapsulation, in which the 1 M KOH solution was added as the electrolyte. The electrochemical measurements of the asymmetric supercapacitor were carried out in a two-electrode cell at room temperature.

#### **Calculations:**

The specific capacitance, can be calculated from the CVs according to the following equation:<sup>1</sup>

$$C = \frac{1}{mv(V_c - V_a)} \int_{V_a}^{V_c} I(V) dV \quad (1)$$

Where C is the specific capacitance (F g<sup>-1</sup>), m is the mass of electroactive materials in the electrode (g), v is the potential scan rate (mV s<sup>-1</sup>), V<sub>c</sub> and V<sub>a</sub> represent the highest and lowest voltages (V), respectively, I(V) is the response current density (A), and V is the potential (V).

The specific capacitance of the electrode can also be calculated from galvanostatic charge-discharge curves by the following formula:<sup>2</sup>

$$C = \frac{I \times \Delta t}{m \times \Delta V} \quad (2)$$

where  $C$  is the specific capacitance ( $\text{F g}^{-1}$ ),  $I$  is the constant discharge current (A),  $\Delta t$  is the discharging time (s),  $m$  is the mass of electroactive materials in the electrode (g), and  $\Delta V$  is the discharging potential range (V).

The energy density ( $E$ ) and power density ( $P$ ) of asymmetric supercapacitors were calculated based on the total mass of the active materials by using the following formulas:

$$E = 0.5C\Delta V^2$$

$$P = E/\Delta t$$

where  $C$  is specific capacitance of asymmetric supercapacitor devices ( $\text{F g}^{-1}$ ) base on the total mass of active materials on both electrodes (g),  $\Delta V$  is the operating potential window, and  $\Delta t$  is the discharge time.

The amount of  $\text{Cu}_3\text{N}$  on the substrate was confirmed by the following method: (1) the P- $\text{Cu}_3\text{N}$  NA/CF was weighed to get the total mass; (2) the P- $\text{Cu}_3\text{N}$  NA/CF was etched with a 0.1 M HCl solution until the colour changed to brass color; (3) the obtained substrate was careful washed with de-ionized water and ethanol several times and dried under flow  $\text{N}_2$ ; (4) the final substrate was weighed to calculate the difference compared to the P- $\text{Cu}_3\text{N}$  NA/CF and the amount of  $\text{Cu}_3\text{N}$  per area was  $2.63 \text{ mg cm}^{-2}$ . The amount of  $\text{CuO}$  ( $3.22 \text{ mg cm}^{-2}$ ) and  $\text{Cu}(\text{OH})_2$  ( $3.71 \text{ mg cm}^{-2}$ ) were also confirmed by the above method.

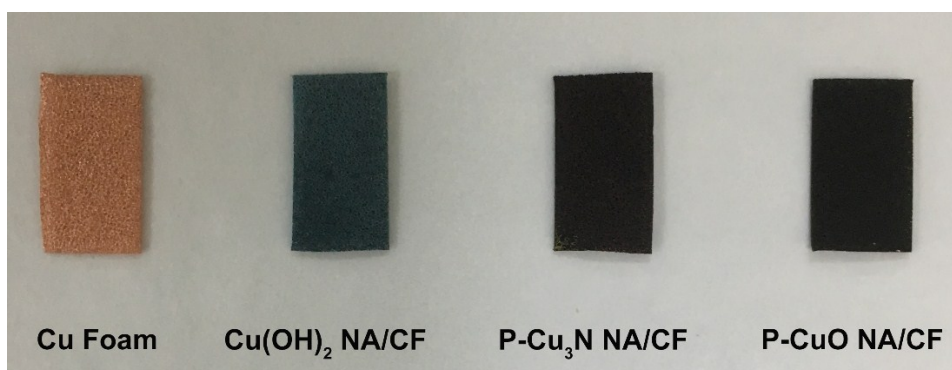


**Fig. S1** photographs of P-Cu<sub>3</sub>N NA/CF, P-CuO NA/CF, Cu(OH)<sub>2</sub> NA/CF, and Cu Foam.

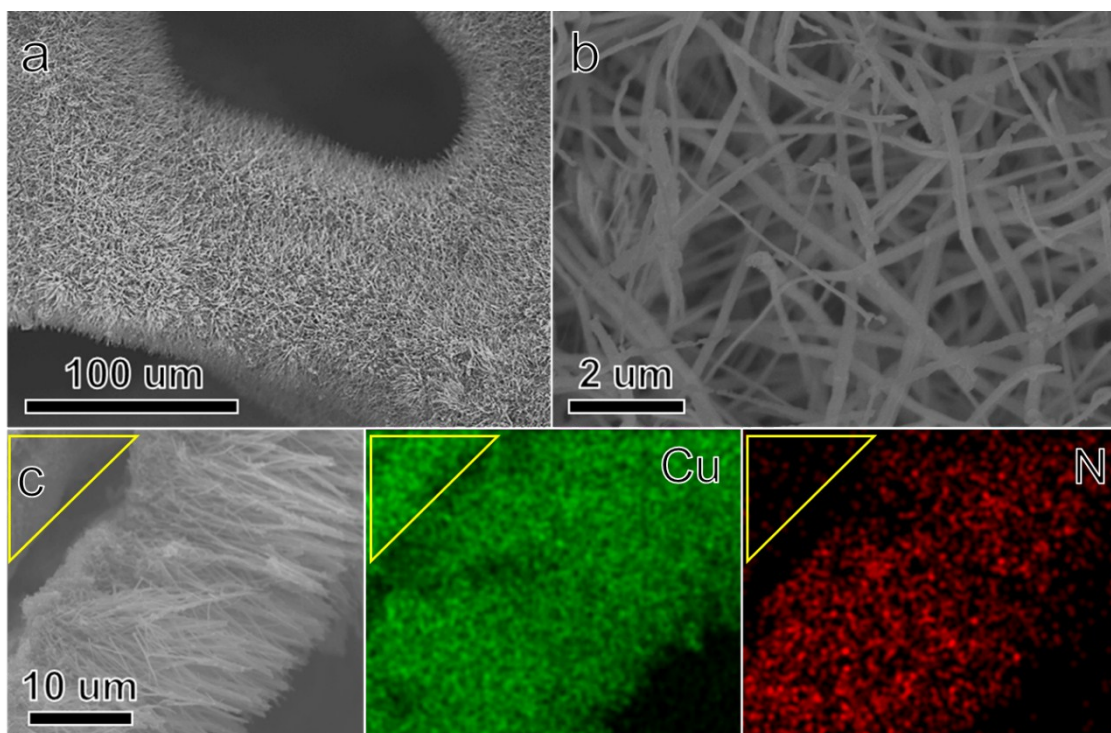


**Fig. S2** (a, b, and c) SEM images of P-Cu<sub>3</sub>N NA/CF and the corresponding SEM EDS element mapping of Cu, and N for P-Cu<sub>3</sub>N NA/CF.

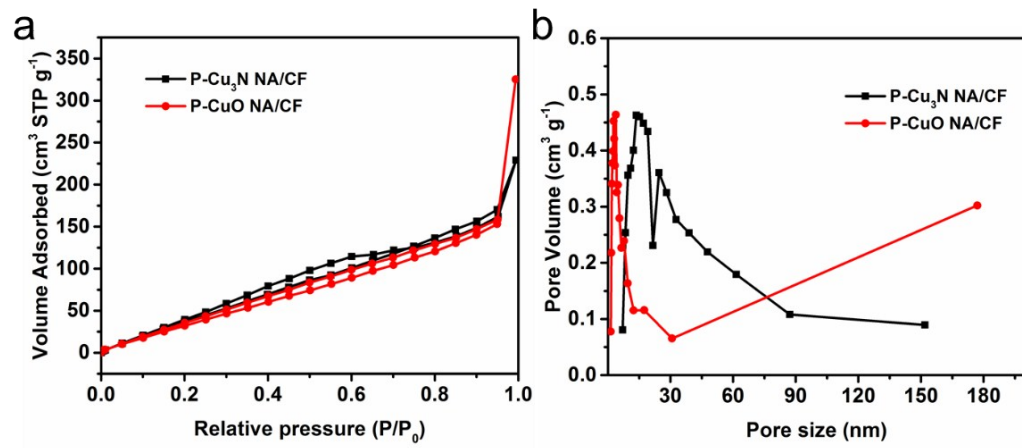


**Fig. S3** (a) The nitrogen adsorption/desorption isotherm and (b) pore size distributions for P-Cu<sub>3</sub>N NA/CF and P-CuO NA/CF.

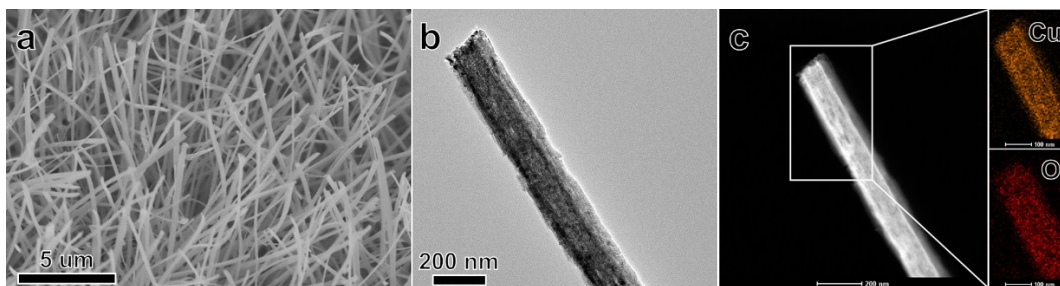


**Fig. S4** (a) The SEM image of P-CuO NA/CF. (b) The TEM image of single porous CuO nanowire. (c) HAADF-STEM image and the corresponding O, and Cu elemental mapping images of single porous CuO nanowire.



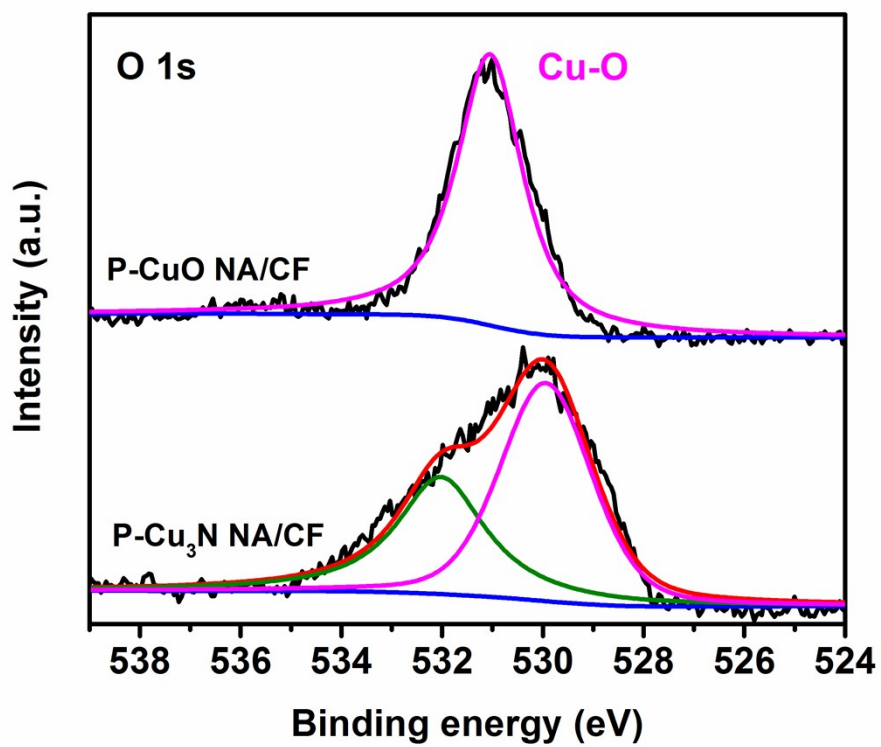


**Fig. S5** The O 1s XPS spectra of P-Cu<sub>3</sub>N NA/CF, and P-CuO NA/CF.

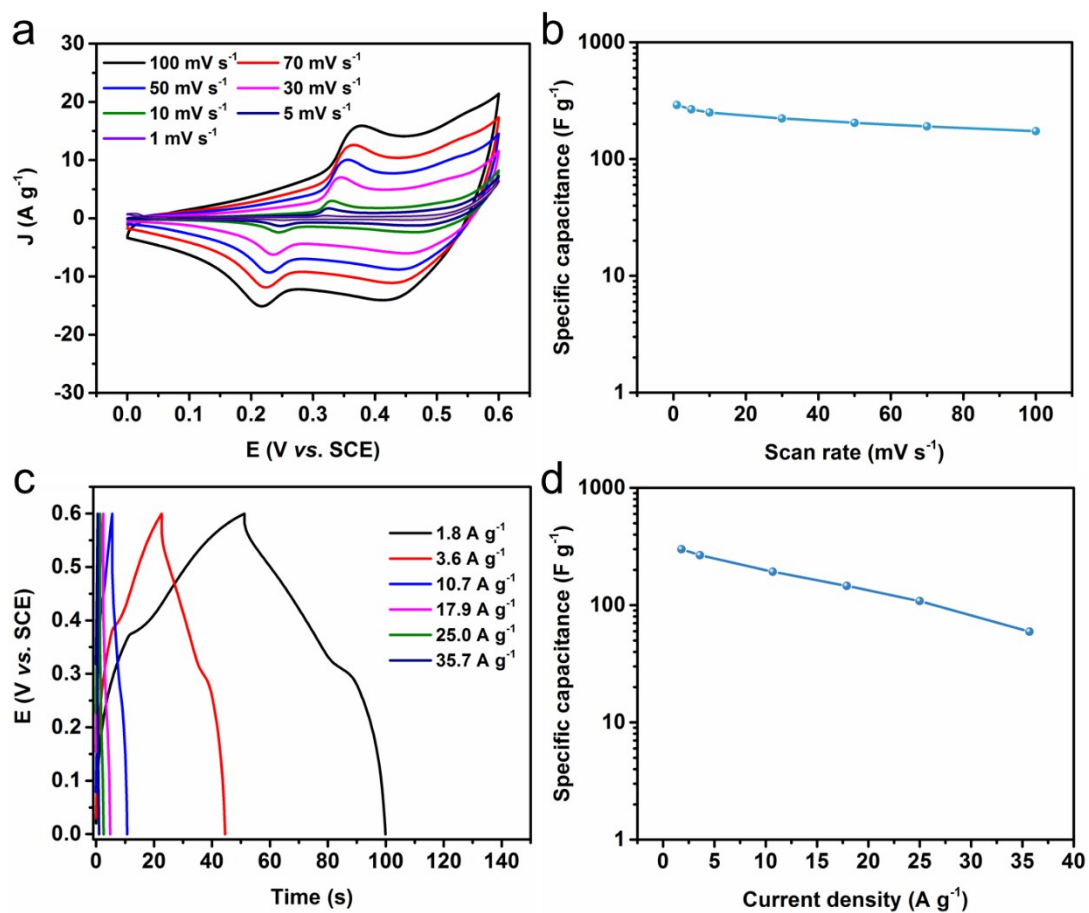


**Fig. S6** (a) CV curves of P-CuO NA/CF at various scan rates in the 1 M KOH solution. (b) Specific capacitance of P-CuO NA/CF as a function of scan rate based on the CVs. (c) Galvanostatic charge-discharge curves of P-CuO NA/CF at various current densities. (d) Specific capacitance of P-CuO NA/CF based on the charge-discharge curves.

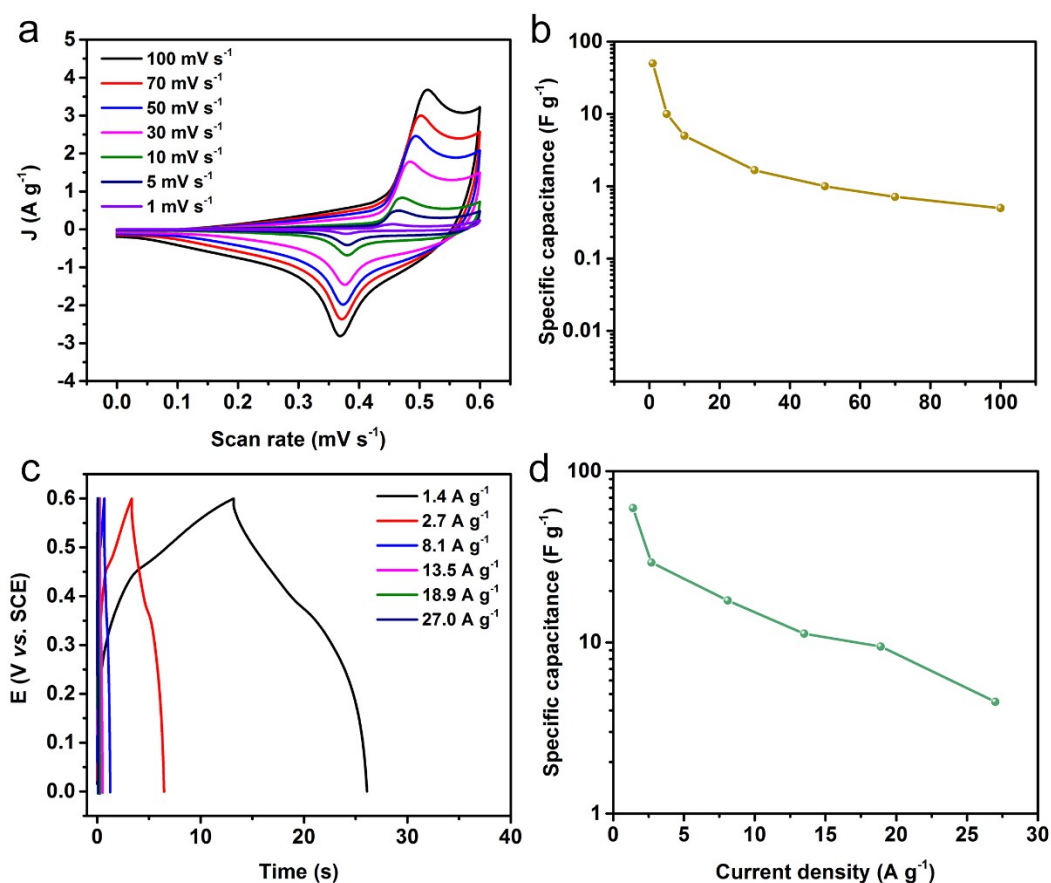


**Fig. S7** (a) CV curves of Cu(OH)<sub>2</sub> NA/CF at various scan rates in the 1 M KOH solution. (b) Specific capacitance of Cu(OH)<sub>2</sub> NA/CF as a function of scan rate based on the CVs. (c) Galvanostatic charge-discharge curves of Cu(OH)<sub>2</sub> NA/CF at various current densities. (d) Specific capacitance of Cu(OH)<sub>2</sub> NA/CF based on the charge-discharge curves.

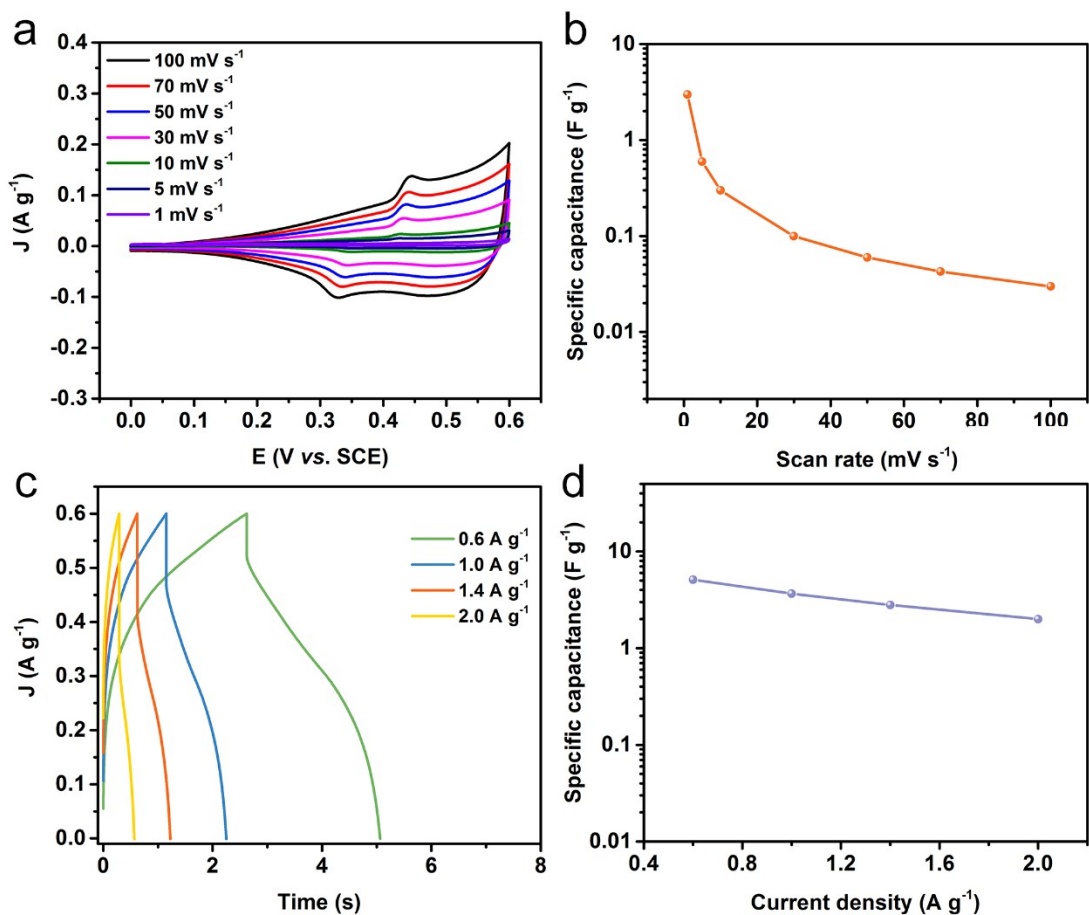


**Fig. S8** (a) CV curves of Cu foam (CF) at various scan rates in the 1 M KOH solution. (b) Specific capacitance of CF as a function of scan rate based on the CVs. (c) Galvanostatic charge-discharge curves of CF at various current densities. (d) Specific capacitance of CF based on the charge-discharge curves.

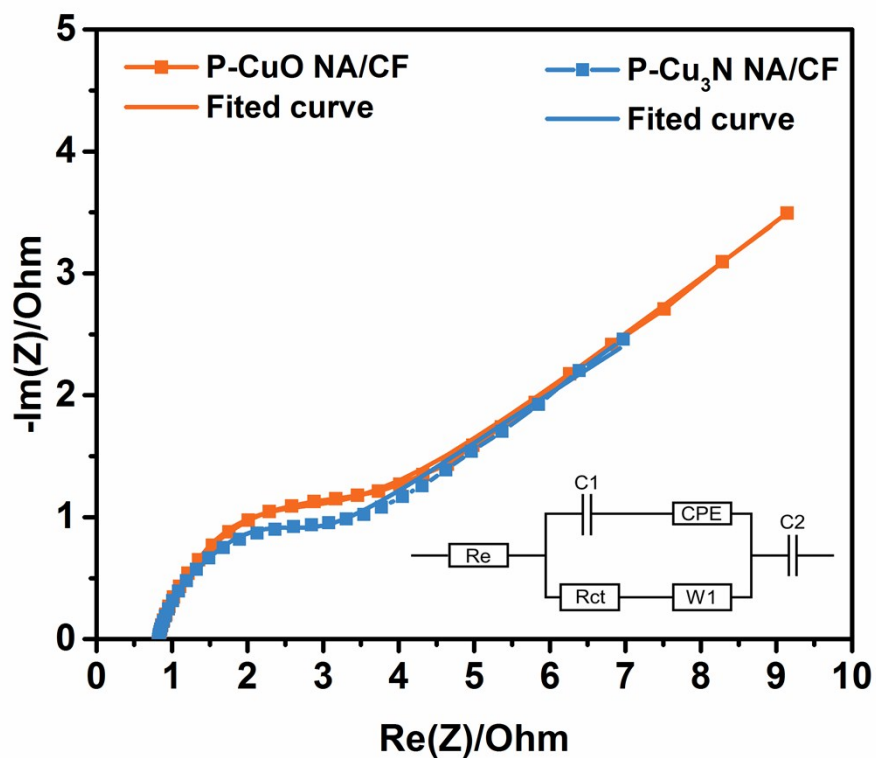


**Fig. S9** Nyquist diagram of the P-Cu<sub>3</sub>N NA/CF, and P-CuO NA/CF carried out at open circuit potential with a frequency ranging from 0.01 Hz to 100 kHz (inset: equivalent circuit diagram).

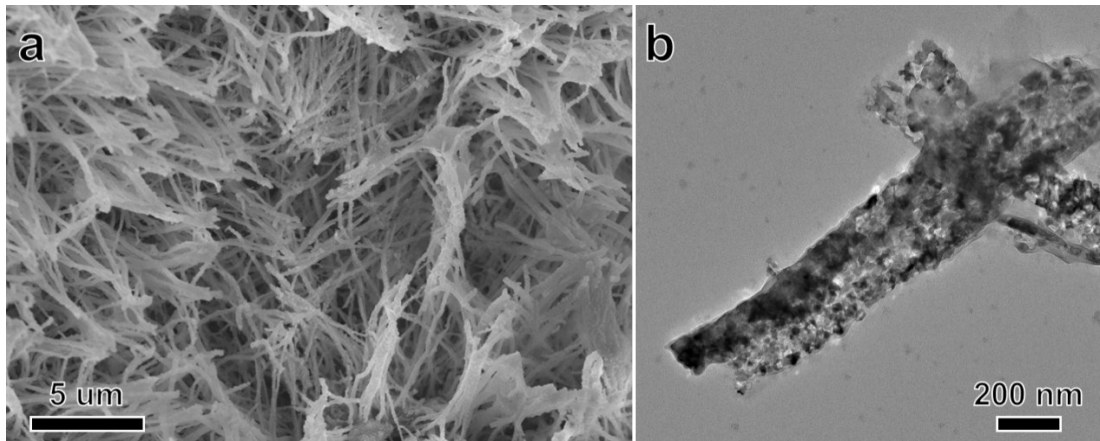


**Fig. S10** The SEM (a) and TEM (b) images of P-Cu<sub>3</sub>N NA/CF after 10000 CV cycles.

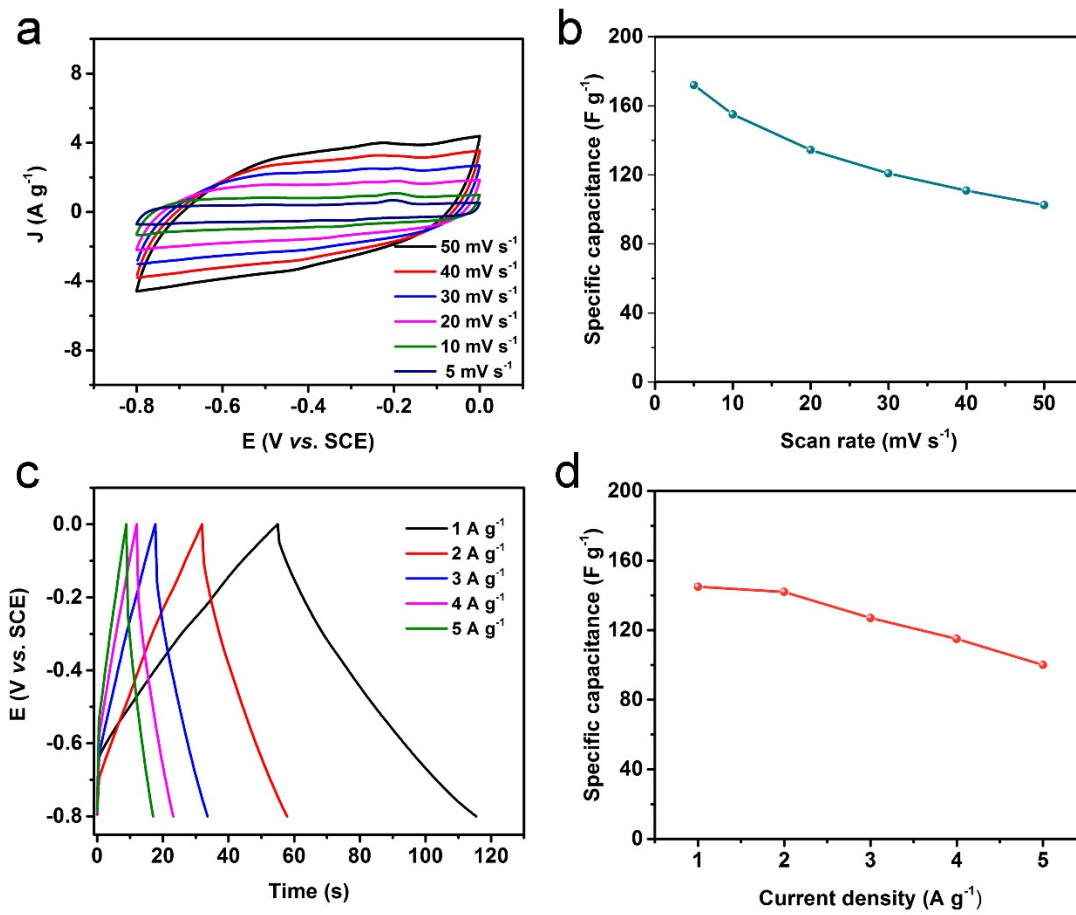


**Fig. S11** (a) CV curves of AC at various scan rates in the 1 M KOH solution. (b) Specific capacitance of AC as a function of scan rate based on the CVs. (c) Galvanostatic charge-discharge curves of AC at various current densities. (d) Specific capacitance of AC based on the charge-discharge curves.

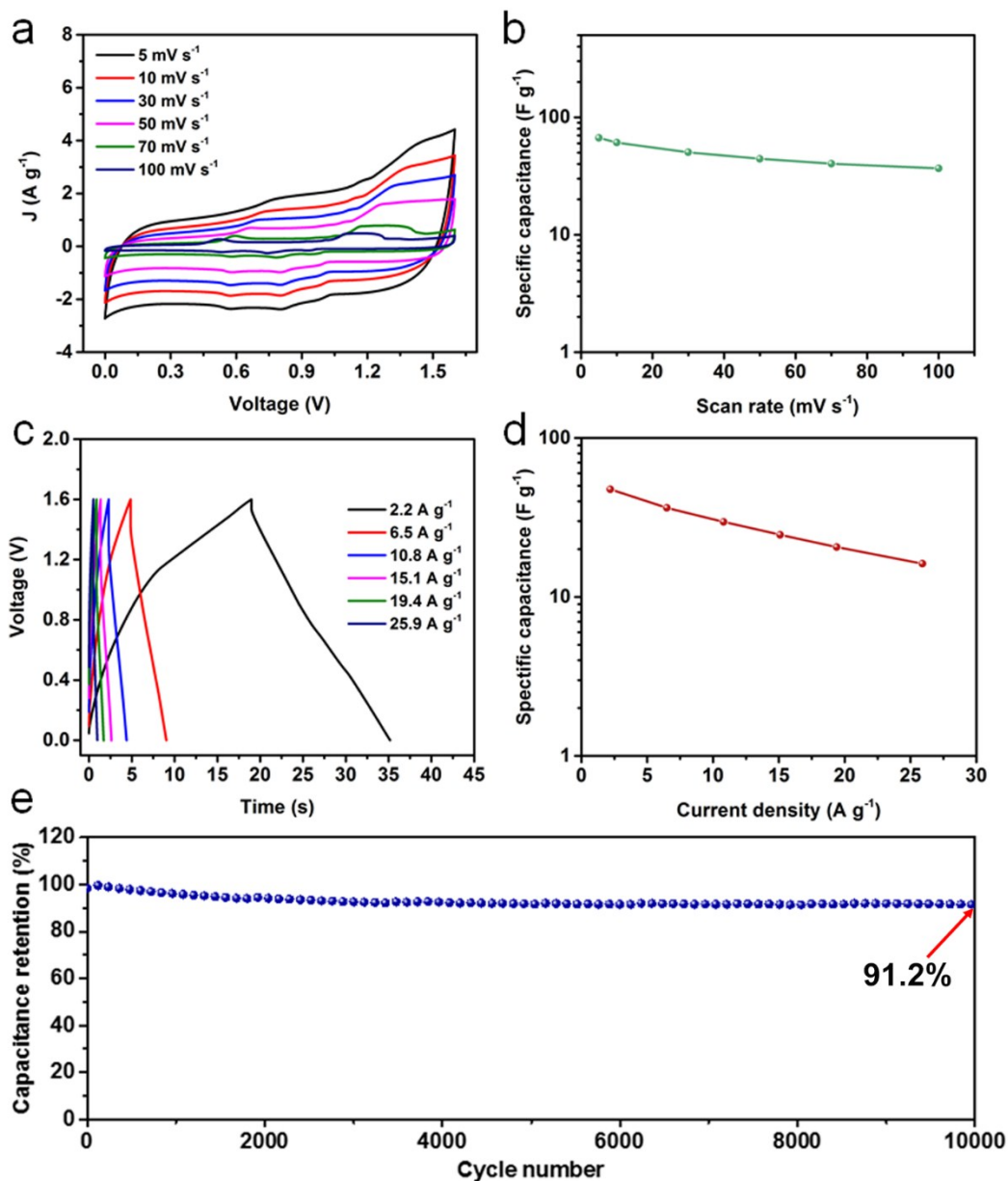


**Fig. S12** Electrochemical performance of the as-fabricated P-Cu<sub>3</sub>N NA/CF//AC asymmetric supercapacitor: (a) CV curves at various scan rates in the 1M KOH solution. (b) Specific capacitance as a function of scan rate based on the CVs. (c) Galvanostatic charge-discharge curves at various current densities. (d) Specific capacitance based on the charge-discharge curves. (e) cycling performance at a current density of 10.8 A g<sup>-1</sup>.



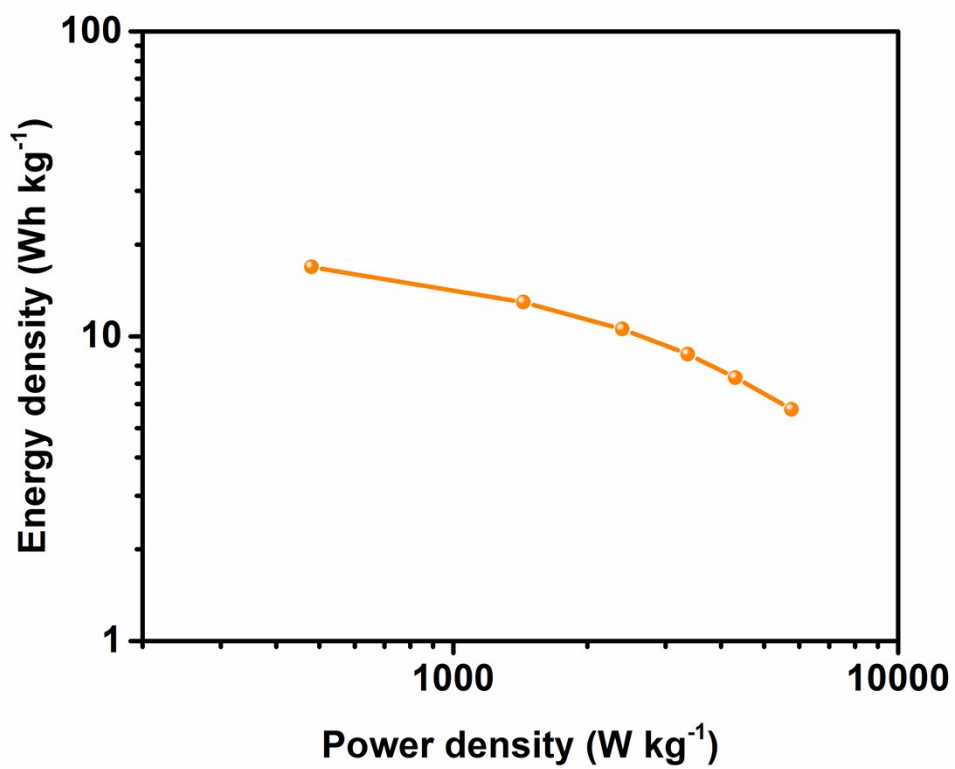


**Fig. S13** Energy density with respect to the power density of the P-Cu<sub>3</sub>N NA/CF//AC asymmetric supecapacitor.

## References

1. Z. Fan, J. Yan, T. Wei, L. Zhi, G. Ning, T. Li and F. Wei, *Adv. Funct. Mater.*, 2011, **21**, 2366.
2. X. Yu, B. Lu and Z. Xu, *Adv. Mater.*, 2014, **26**, 1044.